Proceedings of the 2004 IEEE
International Conference on Robotics & Automation
New Orleans, LA • April 2004

Multi-Contact Compliant Motion Control for Robotic Manipulators

Jaeheung Park,* Rui Cortesão,** and Oussama Khatib*

*Stanford University, Robotics Group, 94305-9010 CA, USA, E-mails: {park73, ok}@robotics.stanford.edu.

**University of Coimbra, Electrical and Computer Engineering Department, Institute of Systems and Robotics (ISR), 3030 Coimbra, Portugal, E-mail: cortesao@isr.uc.pt.

Abstract

The paper describes the formulation of multi-contact compliant motion control. It extends our previous work to non-rigid environments. The contact forces are controlled through Active Observers (AOB), based on the Kalman filter theory. Noise characteristics enter in the control design and are estimated on-line. Experimental results are provided.

1 Introduction

Robotic assembly tasks which require multiple contacts with the environment are present in many industries, demanding advanced control techniques to be efficient. Compliant motion tasks require special attention, since the task constraints change abruptly (between contact and non-contact states) and the model parameters may have wide variations, particularly for very stiff and unstructured environments.

In [3], a general multi-contact motion/force control framework was proposed, which can address tasks beyond the Raibert-Craig model [7]. Additionally, Liu et al [5] proposed an adaptive hybrid control scheme for multiple geometric constraints based on the joint-space orthogonalization. In both of these cases only contact with a rigid environment was considered. However, robotic systems using force sensors in task space always exhibit some compliance. The unified motion/force control framework [4] can be applied to attain compliant contacts, enabling to setup a dynamic equation for the contact model.

Knowing environment parameters, the multi-contact motion/force control formulation decouples into motion and force control by projection matrices for each space. This decentralized control approach is based on feedback linearization techniques, that eliminate nonlinearities and couplings among subsystems. AOBs [1] are used in the force control loop, to cope with modeling errors, including parameter mismatches, noise and external disturbances. Online estimation of the noise variance is applied to cope with a large variation of the noise characteristic. The paper is organized as follows: In Section 2 , the kinematic model for contacts is explained. The dynamic formulation and force control strategy are derived in Section 3 and Section 4, respectively. Experimental results are shown in Section 5. Concluding remarks are discussed in the last section.

2 Multi-Contact model

This section summarizes the Multi-Contact model presented by [3], with the compliant contact model explained in the following sub-section.

When the robotic end-effector is in contact with the environment, the contact constraints can be described by

$$\theta_t = T\beta \quad (1)$$

$$f_c = N\alpha, \quad (2)$$

where θ_t denotes the velocity in the free motion space and f_c is the contact force. When the end-effector has r DOF contact constraints, the column vectors of the matrix N span the contact normal space, i.e.

$$N = [N_1\ N_2\ \cdots\ N_r] \quad (3)$$

and the column vectors of the matrix T span the free motion space, i.e.

$$T = [T_1\ T_2\ \cdots\ T_{6-r}]. \quad (4)$$

Therefore, N is $6 \times r$ and T is $6 \times (6-r)$. α is $r \times 1$ and each element represents the amount of the corresponding contact force/moment N_i at the operational point. β is $(6-r) \times 1$ and each element represents the displacement of the operational point in the corresponding motion space T_i. The matrices N and T can be obtained from the contact geometry [3]. For a point contact model, N in (3) can be represented by

$$N = \begin{bmatrix} \hat{n}_1 & \hat{n}_2 & \cdots & \hat{n}_r \\ \hat{n}_1 \times \vec{l}_1 & \hat{n}_2 \times \vec{l}_2 & \cdots & \hat{n}_r \times \vec{l}_r \end{bmatrix}, \quad (5)$$

where $\hat{n}_i$ is a 3×1 normal vector to the contact surface and $\vec{l}_i$ is a 3×1 vector from the contact point to the operational point. This operational point is the point that is controlled in motion/force and may be different from the contact point (an example is provided for a point contact in a 2-D case at the end of this section). The matrices N and T satisfy

$$N^T T = 0. \tag{6}$$

Projection Matrices

Force and velocity vectors can be decomposed into two spaces using N and T,

$$f = f_1 + f_2 = N\alpha_1 + N'\alpha_2 \tag{7}$$
$$\theta = \theta_1 + \theta_2 = T\beta_1 + T'\beta_2. \tag{8}$$

Having set $N' = T$ and $T' = N$, the projection matrices for

$$f_1 = \Omega_f f,\ f_2 = \bar{\Omega}_f f \tag{9}$$
$$\theta_1 = \Omega_m \theta, \text{ and } \theta_2 = \bar{\Omega}_m \theta \tag{10}$$

can be defined as [3]

$$\Omega_f = N(N^T N)^{-1} N^T = 1 - \bar{\Omega}_f \tag{11}$$
$$\Omega_m = T(T^T T)^{-1} T^T = 1 - \bar{\Omega}_m. \tag{12}$$

These projection matrices have the following properties:

$$\Omega_m = \bar{\Omega}_f, \tag{13}$$
$$\Omega_m \Omega_f = \Omega_f \Omega_m = 0, \tag{14}$$

$$\Omega_m = \Omega_m \Omega_m, \text{ and}$$
$$\Omega_f = \Omega_f \Omega_f. \tag{15}$$

2.1 Modeling for Compliant Point Contacts

A spring model is used in each contact normal space separately, since the environment stiffness is different for each contact. The derivative of the contact force $f_{c,i}$, $\dot{f}_{c,i}$, for each contact normal space is

$$\dot{f}_{c,i} = k_{s,i}\theta_{c,i}, \tag{16}$$

where i denotes each contact and $\theta_{c,i}$ is the velocity of the operational point in the contact normal space. $k_{s,i}$ represents the operational point stiffness, which may be different from the contact point stiffness k_{env}. It is simply derived from the geometry of a contact point, an operational point and a contact normal vector. It is given by

$$k_{s,i} = k_{\text{env}} \left(1 + |\vec{l} \times \hat{n}|^2\right). \tag{17}$$

The magnitude of $k_{s,i}$ can vary from k_{env} to $k_{env}(1 + l^2)$ depending on the configuration of the object with respect to the contact surface.

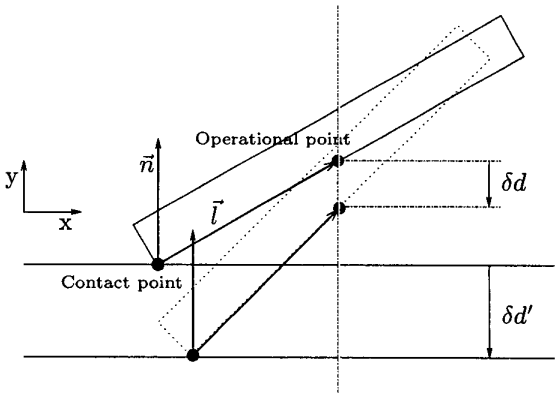

***Figure 1:** 2D Example.*

2.2 2D Example: Planar Case

This section presents a 2D example showing how the contact normal space N can be expressed. The derivation of the operational space stiffness from the contact stiffness is also discussed. The operational point has 3 DOF, which are translation in x and y directions and rotation around the z direction. In Figure 1, the contact normal vector $\hat{n} = [0\ 1]^T$. N can be obtained from (5),

$$N = \begin{bmatrix} \hat{n} \\ \hat{n} \times \vec{l} \end{bmatrix} = \begin{bmatrix} 0 \\ 1 \\ -l \sin\gamma \end{bmatrix}, \tag{18}$$

where $\hat{n} \times \vec{l}$ points to $-\hat{z}$, $|\vec{l}| = l$ and $\angle(\hat{n}, \vec{l}) = \gamma$ [rad]. When the operational point has a small displacement $N\delta d$,i.e, the operational point moves δd in $\hat{y}$ and rotates $l\delta d \sin\gamma$ around $-\hat{z}$, it creates a motion of the contact point in $\hat{y}$ given by $\delta d' = \delta d(1 + l^2 \sin^2\gamma)$. This motion originates the contact force

$$k_{\text{env}}\ \delta d' = k_{\text{env}}(1 + l^2 \sin^2\gamma)\delta d. \tag{19}$$

Therefore, the force increment due to the small displacement $N\delta d$, δf_c, can be represented by

$$\delta f_c = k_{env}(1 + l^2 \sin^2\gamma)\delta d \begin{bmatrix} 0 \\ 1 \\ -l \sin\gamma \end{bmatrix} = k_{env}(1 + l^2 \sin^2\gamma)\delta d_c, \tag{20}$$

where $\delta d_c = N\delta d$. The effective stiffness is given by

$$k_s = k_{env}(1 + l^2 \sin^2\gamma). \tag{21}$$

The meaning of Ω_f and Ω_m can be illustrated in the case where $l = \sqrt{2}$ and $\gamma = 45^o$:

$$\begin{aligned} N &= [0 \quad 1 \quad -1]^T \\ \Omega_f &= \begin{bmatrix} 0 & 0 & 0 \\ 0 & 0.5 & -0.5 \\ 0 & -0.5 & 0.5 \end{bmatrix} \\ \Omega_m &= \begin{bmatrix} 1 & 0 & 0 \\ 0 & 0.5 & 0.5 \\ 0 & 0.5 & 0.5 \end{bmatrix}. \end{aligned} \tag{22}$$

The projection matrices are used in the following section to decouple motion control from force control. The acceleration filtered by Ω_m will generate no acceleration of the contact point; thus, the contact force is independent upon the motion control, which has a desired acceleration filtered by Ω_m.

3 Control Design

The manipulator dynamics can be expressed using the Operational Space Formulation [4] as follows:

$$\Lambda_o(x)\dot{\theta} + \mu_o(x,\theta) + p_o(x) + f_c = F, \tag{23}$$

where x is an operational space coordinate vector and θ denotes the instantaneous linear/angular velocity of the end-effector. $\mu_o(x,\theta)$ represents Coriolis and Centripetal forces and $p_o(x)$ is gravity force. f_c is contact force with environment and F is the commanding force in Operational Space. Torque $\Gamma = J^T F$ will be applied to the manipulator. If F is given by (the symbol $\hat{}$ means estimate)

$$F = f^*_{com} + \hat{\mu}_o(x,\theta) + \hat{p}_o(x) + \hat{f}_c{}^1. \tag{24}$$

The resulting equations of motion are

$$\Lambda_o \dot{\theta} = f^*_{com}. \tag{25}$$

The commanded force f^*_{com} is composed by the motion control part f^*_t and also by the contact force control part f^*_c, i.e.

$$f^*_{com} = \Lambda_o \Omega_m f^*_t + \Lambda_o \Omega_f f^*_c. \tag{26}$$

¿From (25) and (26),

$$\dot{\theta} = \Omega_m f^*_t + \Omega_f f^*_c. \tag{27}$$

Therefore, the motion space and contact normal space are decoupled as can be shown

$$\dot{\theta}_t = \Omega_m \dot{\theta} = \Omega_m f^*_t \tag{28}$$

$$\dot{\theta}_c = \Omega_f \dot{\theta} = \Omega_f f^*_c. \tag{29}$$

The design of f^*_t and f^*_c will be discussed in the sequel.

[1] $\hat{f}_c$ is obtained from the estimated contact forces in the AOB.

3.1 Motion Control

The desired position of the end-effector is provided without considering contacts, such as a motion from a user in teleoperation or a given smooth trajectory. f^*_t is designed with a PD controller.

Since f^*_t is pre-multiplied by the projection matrix Ω_m, the motion control will not affect the contact forces.

3.2 Force Control

The design of the force control part f^*_c should be done explicitly in the contact force space since the desired amount of contact force for each point is specified. Since $f_c = N\alpha$, a feedback control is designed for each contact force space, the column spaces of N.

$$\begin{aligned} f^*_c &= N\alpha^*_c \\ \alpha^*_c &= [\alpha^*_{c,1}, \alpha^*_{c,2}, ..., \alpha^*_{c,r}]^T. \end{aligned} \tag{30}$$

Then, with (29) and (16),

$$\ddot{f}_{c,i} = k_{s,i} f^*_{c,i} \quad \text{and} \quad \ddot{\alpha}_{c,i} = k_{s,i} \alpha^*_{c,i}. \tag{31}$$

where i denotes each contact. $\alpha_{c,i}$ and $k_{s,i}$ are scalar. The force control design is described in the following section.

4 Force Control Design

The force control is implemented for a decoupled subsystem (31). With an additional damping $K_2\theta_{c,i}$ to $f^*_{c,i}$ for better stability and a small system input delay T_d, the overall system can be approximated by

$$G(s) = \frac{k_{s,i} e^{-sT_d}}{s(s+K_2)}, \tag{32}$$

where K_2 is a positive scalar. The discretized state space form of the system equation (32) is

$$\begin{aligned} x_{r,k} &= \Phi_r x_{r,k-1} + \Gamma_r u_{k-1} \\ y_k &= C_r x_{r,k}. \end{aligned} \tag{33}$$

With input disturbance estimate p_k,

$$\begin{aligned} \begin{bmatrix} x_{r,k} \\ p_k \end{bmatrix} &= \begin{bmatrix} \Phi_r & \Gamma_r \\ 0 & 1 \end{bmatrix} \begin{bmatrix} x_{r,k-1} \\ p_{k-1} \end{bmatrix} \\ &\quad + \begin{bmatrix} \Gamma_r \\ 0 \end{bmatrix} u_{k-1} + \xi_{x_k} \\ y_k &= C_a [x_{r,k-1} \quad p_{k-1}]^T + \eta_k, \end{aligned} \tag{34}$$

where

$$C_a = [C_r \quad 0]. \tag{35}$$

A full state feedback is implemented using Pole Placement method(Ackermann's formula), with which L_r is designed; thus the input to system is

$$u_{k-1} = r_{k-1} - [L_r \quad 1] \begin{bmatrix} \hat{x}_{r,k-1} \\ \hat{p}_{k-1} \end{bmatrix}. \tag{36}$$

The stochastic inputs ξ_k and η_k are model and measurement uncertainties. The state estimation is based on (34) and (36).

$$\begin{bmatrix} \hat{x}_{r,k} \\ \hat{p}_k \end{bmatrix} = \begin{bmatrix} \Phi_r - \Gamma_r L_r & 0 \\ 0 & 1 \end{bmatrix} \begin{bmatrix} \hat{x}_{r,k-1} \\ \hat{p}_{k-1} \end{bmatrix} + \begin{bmatrix} \Gamma_r \\ 0 \end{bmatrix} r_{k-1} + K_k(y_k - \hat{y}_k) \tag{37}$$

with

$$\hat{y}_k = C_a \left(\begin{bmatrix} \Phi_r - \Gamma_r L_r & 0 \\ 0 & 1 \end{bmatrix} \begin{bmatrix} \hat{x}_{r,k-1} \\ \hat{p}_{k-1} \end{bmatrix} + \begin{bmatrix} \Gamma_r \\ 0 \end{bmatrix} r_{k-1} \right). \tag{38}$$

The Kalman gain K_k is

$$K_k = P_{1k} C_a^T [C_a P_{1k} C_a^T + R_k]^{-1} \tag{39}$$

with

$$\begin{aligned} P_{1k} &= \Phi_n P_{k-1} \Phi_n^T + Q_k \\ P_k &= P_{1k} - K_k C_a P_{1k}. \end{aligned} \tag{40}$$

Φ_n is the augmented open loop matrix, i.e,

$$\Phi_n = \begin{bmatrix} \Phi_r & \Gamma_r \\ 0 & 1 \end{bmatrix}. \tag{41}$$

Q_k is the system noise matrix representing model uncertainty. R_k is the measurement noise variance matrix, which is updated on-line as will be discussed in the next section. P_k is the mean square error matrix of the states. More details in implementation and robustness analysis can be referred to [2].

4.1 Noise Variance Characteristics in Contact Motion

The noise variance for the measurement force influences the estimation strategy. If the noise increases, the force estimation should rely more on the force model rather than measured data. Experimental tests have shown that the measurement noise varies while the robot is moving in contact mainly due to the friction and the amount of contact force. Therefore, on-line noise identification has been performed to adapt the state estimation.

4.2 Noise Variance Estimation

Maybeck [6] used the maximum likelihood equations to estimate the measurement covariance matrix. The method optimizes the estimation of the measurement variance with the model and measurements. However, this approach is too sensitive to disturbances, such as in the case that the robot starts or stops a motion, or forces are applied to other contact points. To cope with this difficulty, another approach is applied.

Low frequency values of the force generated by the controller or by external disturbances can corrupt the noise estimation. Therefore, a high-pass filter is used for the measured force data before noise analysis,

$$\alpha_f(z) = G_f(z)\alpha(z), \tag{42}$$

where $G_f(z)$ is the discrete time first order high-pass filter which has a zero and a pole with DC gain of 1.0. $\alpha(z)$ is the measured contact force for each contact force space. The zero and the pole have been chosen as 3 [Hz] and 60 [Hz], respectively, according to our closed loop design specifications. The estimation of the measurement noise, $\hat{R}(t_i)$, is given by

$$\hat{R}(t_i) = \frac{1}{N} \sum_{j=i-N+1}^{i} \{[\alpha_f(t_j) - \bar{\alpha}_f][\alpha_f(t_j) - \bar{\alpha}_f]^T\}, \tag{43}$$

where $\bar{\alpha}_f$ is the mean of the filtered force over a time window, i.e.

$$\bar{\alpha}_f = \frac{1}{N} \sum_{j=i-N+1}^{i} \alpha_f(t_j). \tag{44}$$

50 samples have been used in the experiments.

5 Experiments

5.1 System Setup

The system setup represented in Figure 2 consists of a PUMA robot, a table and a vertical board. The vertical board has a 90 deg angle with the table. The computer runs at 500 [Hz] with the QNX operating system. Contact forces are measured by a JR3 force sensor.

As can be seen in Figure 2, two rigid bars have contacts with a table and a vertical board. Step functions are commanded for two contact forces. The motion in the other direction tracks a sinusoidal input while the orientation of the wrist remains fixed.

5.2 Experiments and Results

The motion control is designed to be critically damped with a natural frequency $\omega_n = 30$(rad/sec).

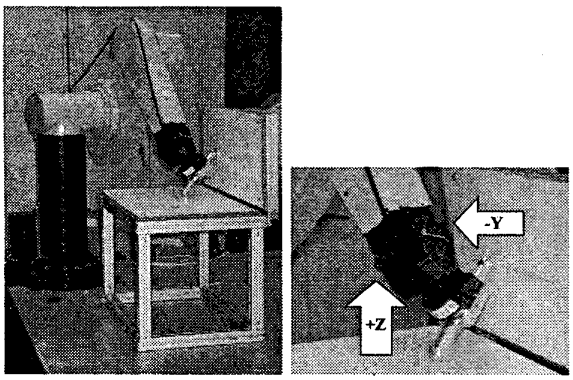

(a) (b)

Figure 2: *System Setup.*

The full state feedback gain L_r for the force control is set to have a time constant of 0.02 [sec].

The system noise matrix is $Q_k = 10^{-3} I_{6\times6}$ and $P_0 = 10^{-3} I_{6\times6}$. The measurement noise R_k is calculated on-line.

Figure 3 and Figure 4 show the contact forces and the estimated forces over time. The translational motion in the x direction is represented in Figure 5. The manipulator starts with no motion (range [160-190] [s]). In this case, step forces (10 [N] and 15 [N]) have been applied to both z and y directions. The operational point of the end-effector (the wrist point) starts moving at 190 [s] in in the x direction.

The contact force follows the commanded force with the designed time constant. Figure 6 shows the force variance for each contact. The variance is about 0.6 in a static situation, increasing to about 100.0 when the manipulator moves. Although the noise characteristic varies a lot, the on-line noise estimation is able to properly adapt the control such that the contact forces are not too affected by the motion. Starting the motion of the end-effector disturbs both contact forces significantly at about 195, 205, and 217 [s].

The pre-estimated value of $k_{s,i} = 6,000N/m$ is used for the stiffnesses of both the table and the vertical board. Although this value is not perfect, the robust force control with a modified Kalman estimation (AOB) compensates modeling errors, guaranteeing the desired force dynamics.

It should be mentioned that on-line noise variance estimation plays a critical role in the control performance. If no on-line estimation is done, the control only works if the robot does not move. The motion generates too much noise in the force data, leading

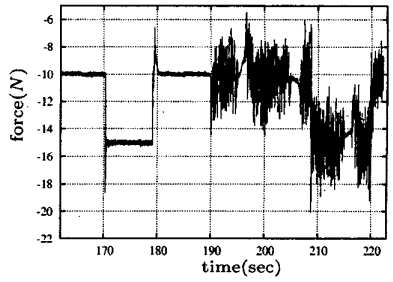

(a) Measured force of the first contact. z direction.

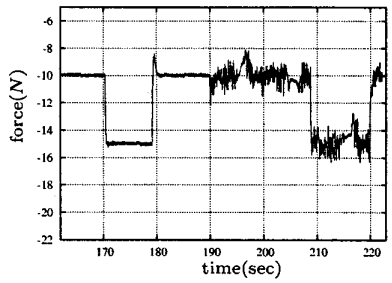

(b) Estimated force of the first contact. z direction.

Figure 3: *Measured and Estimated forces in contact with the table.*

the system to instability. Without the high-pass filter before the variance computation, the system responds much slower to disturbances.

6 Conclusion

A multi-contact compliant motion design has been introduced, based on the operational space formalism and AOBs. This general formulation can achieve tasks with multiple contacts, which cannot be described by the Raibert-Craig model. A method for on-line measurement noise estimation has been proposed. Experiments with a PUMA robot for two contact points have been analyzed. The nonlinear and coupled manipulator dynamics is transformed into decoupled linear sub-systems through feedback linearization techniques. These decoupled sub-systems are controlled by a state-space control scheme with a modified adaptive Kalman estimator(AOB). The AOB compensates modeling errors generated from the overall formulation.

References

[1] R. Cortesão. *Kalman Techniques for Intelligent Control Systems: Theory and Robotic Experiments.* PhD thesis, University of Coimbra, 2002.

[2] R. Cortesão, J. Park, and O. Khatib. Real-time adaptive control for haptic manipulation with active ob-

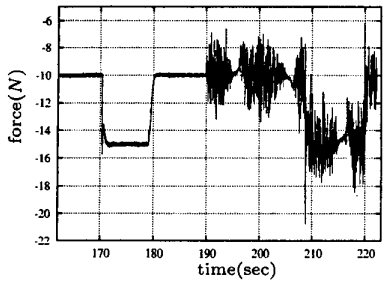

(a) Measured force of the second contact. y direction.

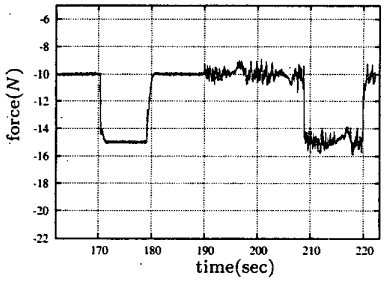

(b) Estimated force of the second contact: y direction.

Figure 4: *Measured and Estimated forces in contact with the vertical board.*

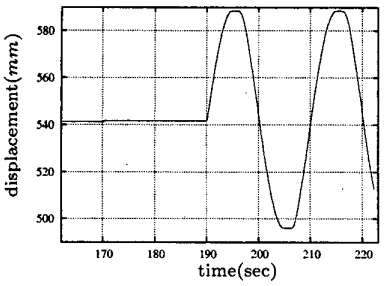

Figure 5: *Wrist translational motion in x direction.*

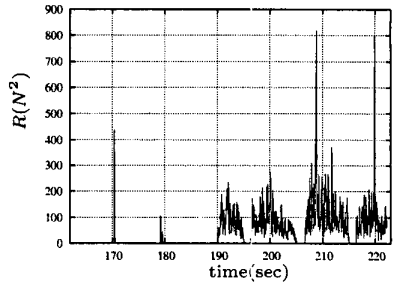

(a) Noise Covariance Estimation for the first contact force.

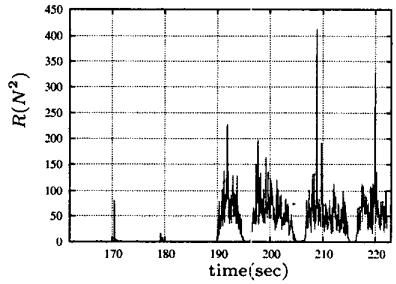

(b) Noise Covariance Estimation for the second contact force.

Figure 6: *Noise Variance Estimations.*

servers. In *Proc. of the Int. Conf. on Intelligent Robots and Systems (IROS)*, Las Vegas, 2003.

[3] Roy Featherstone, Stef Sonck Thiebaut, and Oussama Khatib. A general contact model for dynamically-decoupled force/motion control. In *Proc. of the Int. Conf. on Robots and Automation*, pages 3281–3286, Detroit, Michigan, 1999.

[4] O. Khatib. A unified approach for motion and force control of robot manipulators: The operational space formulation. *Int. J. on Robotics and Automation*, 3(1):43–53, February 1987.

[5] Yun-Hui Liu, Kosei Kitagaki, Tsukasa Ogasawara, and Suguru Arimoto. Model-based adaptive hybrid control for manipulators under multiple geometric constraints. *IEEE Trans. on Control Systems Technology*, 7(1):97–109, January 1999.

[6] Peter S. Maybeck. *Stochastic Models, Estimation and Control (Volume 2)*, volume 141-2 of *Mathematics In Science and Engineering*. Academic Press, 1982. (Edited by R. Bellman).

[7] M. H. Raibert and J. J. Craig. Hybrid position/force control of manipulators. *ASME Journal of Dynamic Systems, Measurement and Control*, 103(2):126–133, June 1981.